MJFAS MALAYSIAN JOURNAL OF FUNDAMENTAL AND APPLIED SCIENCES
PRINT ISSN: 2289-5981 | ONLINE ISSN: 2289-599X

RESEARCH ARTICLE

Synthesis and optimization of nano-sized bacterial-based violacein pigment using response surface methodology

Haryani Mohd Yatim, Claira Arul Aruldass, Mohd Amir Asyraf Mohd Hamzah, Wan Azlina Ahmad, Siti Aminah Setu*

Department of Chemistry, Faculty of Science, Universiti Teknologi Malaysia, 81310 UTM Johor Bahru, Johor, Malaysia

** Corresponding author: sitiaminahsetu@kimia.fs.utm.my*

Article history
Received 26 August 2018
Revised 4 April 2019
Accepted 15 April 2019
Published Online 3 December 2019

Abstract

Violacein from *Chromobacterium violaceum* has raised the enthusiasm of researchers in conducting comprehensive studies on these pigments due to their diverse biological activities including antibacterial and antioxidant properties. However, a limitation related with the solubility of the violacein pigment, by which it is commonly dissolved in toxic solvents such as dimethyl sulfoxide and methanol instead of being soluble in biological fluids and water. Hence, this study provides a method to synthesis the violacein pigment in nanoscale through an encapsulation technique using chitosan-tripolyphosphate (Cs-TPP) nanoparticles. The synthesis of nanoparticles in this study involved ionic gelation between chitosan and tripolyphosphate (TPP), in which several parameters were taken into consideration in order to control the size and dispersion stability of the violacein pigment in the suspension. Preparation parameters, including the concentration of chitosan, TPP and pigment as well as the mass ratio of chitosan to TPP, were optimized using Response Surface Methodology (RSM). Minimum particle size of 149.0 nm with zeta potential of +23.40 mV was obtained at the optimal formulations of 2.33 mg/mL of chitosan, 1.5 mg/mL of TPP, and 1 ppm of violacein pigment and at mass ratio of chitosan:TPP of 7:1. This nano-sized violacein pigment is expected to be applied as safe additive, colorant, and therapeutic agents. Meanwhile, RSM in the study could provide the optimal formulations for producing stable nano-sized violacein pigment.

***Keywords*:** Bacterial-based violacein pigment; response surface methodology, pigment nanoparticles

INTRODUCTION

Natural pigments have been widely utilized in various industries in high demands since the public become more aware with the toxicity, carcinogenicity, and mutagenicity of its rival, synthetic pigments. These pigments contain chromophores which are important for appearance of color in animals, plants, and bacteria [1]. Although all taxonomic groups are known to produce natural pigments, bacteria are recognized as potential source of pigment owing to their distinctive advantages such as short life cycle, availability irrespective of seasons and geographical conditions, able to produce variety of colors and shades, as well as accessibility of production and downstream processing [2].

Violacein, 3-[1,2-dihydro-5-(5-hidroxy-1*H*-indol-3-yl)-2-oxo-3*H*-pyrrol-3-ilydene]-1,3-dihydro-2*H*-indol-2-one (Figure 1) is a violacein pigment produced by *Chromobacterium violaceum* in the presence of free oxygen [3]. This unique violacein pigment has propelled the enthusiasm among researchers due to its antitumoral [4], antiviral [5], antifungal [6], antimicrobial [7], and anticancer activities [8].

However, violacein has limited solubility in water and biological fluids and commonly dissolved in toxic solvents such as dimethyl sulfoxide and methanol [9]. Nanoencapsulation has become one of the recent emerging approach of encapsulation as nanoparticles can be conformed to envelop or reservoirs of bioactive particles which are trapped and released from the large surface area [10]. Martins *et al.* [9] overcome the limitation solubility of violacein by encapsulating the violacein into polymeric poly-($_{D,L}$-lactide-co-glycolide) acid (PLGA) nanoparticles *via* nanoprecipitation method [9]. However, the loaded violacein-PLGA nanoparticles had negatively-charged outer surfaces, which restrict the interactions with negatively-charged cell membrane of bacteria [11]. This interferes the determination of antibacterial activity of the violacein against microorganism.

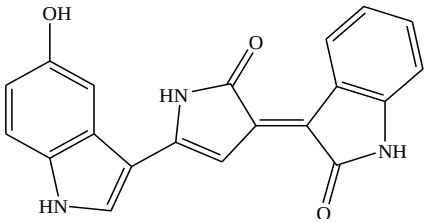

Figure 1 Chemical structure of violacein [3].

Alternatively, chitosan nanoparticles are taken into consideration since it has been widely studied for pharmaceutical and biomedical applications particularly in the drug delivery systems such as dexamethasone [11], indomethacin [12], quetiapine fumarate [13], methotrexate [14], sumatriptan succinate [15], and dextran-doxorubicin conjugate [16]. Properties of the chitosan including mucoadhesive, biocompatible, biodegradable, non-toxic, and possessing antimicrobial activity had made it as desirable polymer and encapsulating agent in drug delivery system [17]. Various encapsulation techniques have been explored and applied such as spray drying, ionic gelation, coacervation, liposome entrapment, and emulsion phase separation [18]. Ionic gelation has several advantages over the other methods as this

technique requires simple and mild conditions, does not involve high temperature or the use of organic solvents, and also prevents the possibility of damage to drugs, especially biological agents [12,15,17,18]. However, this technique is highly sensitive to numerous environmental variables, component, and process conditions [14]. The chitosan nanoparticles are known to aggregate or fuse directly after preparation and have a limited stability during storage. In previous studies, several parameters have been considered for assessing the interaction effects upon the responses such as particle size, polydispersity index, encapsulation efficiency, and zeta potential for optimization of chitosan nanoparticles. Abul Kalam *et al.* [12] reported on the interaction effect of three parameters of nanoparticles which are chitosan concentration, tripolyphosphate (TPP) concentration, and stirring rate to optimize the encapsulation of indomethacin to chitosan nanoparticles. The authors found that these parameters have synergistic effect on the size of the nanoparticles [12]. de Pinho *et al.* [19] optimized the chitosan nanoparticles formulation by analyzing the effect of pH, chitosan:TPP ratio, and acetic acid concentration in particle size and zeta potential of chitosan nanoparticles [19]. Therefore, it is important for researchers to study the optimization of preparation parameters to acquire the optimum conditions for attaining nano-sized encapsulated particles with low polydispersity index and high zeta potential.

In the past, the optimization of chitosan nanoparticles using Response Surface Methodology (RSM) was conducted to produce stable particles [12–14]. RSM is a constructive tool that employs the combination of mathematical and statistical techniques that is used for designing, developing, optimizing, formulating, and improving processes [20]. Thus in present study, optimal conditions for the preparation of nano-sized violacein through encapsulation with chitosan nanoparticles by employing 3-factor 3-level Box–Behnken experimental design was investigated. Several parameters were optimized to produce nano-sized violacein with small particle size and high zeta potential which were concentration of chitosan, concentration of TPP, chitosan:TPP mass ratio, and concentration of violacein

EXPERIMENTAL

Materials

Low molecular weight chitosan and sodium tripolyphosphate were purchased from Sigma-Aldrich (USA). Sodium hydroxide and Tween 80 was purchased from Merck (Germany). Glacial acetic acid and other chemicals used were of analytical grade while ethylacetate and acetone used for extraction of pigments were of industrial grade. Ultrapure water was obtained by Milli-Q® water purifier (Millipore, France).

Production of crude violacein pigment in 5-L bioreactor

Chromobacterium violaceum UTM5 (GenBank accession no. HM132057), a violacein pigmented bacterial strain was obtained from the stock which have been collected, isolated, and prepared by UTM Bacterial Technology Research Group [7,21]. In this study, crude violacein was produced using liquid pineapple waste (LPW) in accordance with method from Aruldass *et al.* [7] as this approach highlighted potential low cost growth medium for the large-scale production process [7]. *C. violaceum* UTM5 was inoculated into a series of 250 mL Erlenmeyer flasks containing 62.5 mL nutrient broth (NB) and incubated at 30 °C (Memmert, United Kingdom) for 24 hours in the dark under static condition. Then, 50 mL inoculum (10 % (v/v)) was transferred into a 2-L Erlenmeyer flask containing 450 mL NB along with 150 mg/L L-tryptophan (from L-tryptophan stock solution; 1000 mg/L) and incubated at 30 °C (Memmert, United Kingdom) for 24 hours in the same aforementioned condition. Next, the culture (10 % (v/v)) with 5×10^7 CFU/mL, 500 mL was transferred into a 5-L bioreactor (Biotron Liflus GX 7 L, Korea) containing 4.5 L of 10 % (v/v; in sterile reverse osmosis water) LPW and cultivated for 24 hours under the following conditions: 30 °C, 200 rpm, aeration rate 3 L/min, initial pH of 7.0, and with an addition of Antifoam A (Sigma, Germany). Crude violacein was extracted using ethyl acetate (J.T. Baker, USA) at the culture to solvent ratio of 4:1. Next, the extract was concentrated using a rotary evaporator (Büchi, Switzerland) at 50 °C.

Synthesis of violacein pigment nanoparticles

Violacein nanoparticles were synthesized by encapsulating the violacein with chitosan using ionic gelation technique. Preparation of The violacein nanoparticles was prepared by following the methods explained by Aruldass *et al.* [7] and Hussain and Sahudin [22] with some modifications [7,22]. Chitosan was dissolved in 1 % (v/v) acetic acid and left stirred overnight. Chitosan solution was filtered through a 0.45 µm syringe filter to remove undissolved residues. The concentration of chitosan solution ranged from 1–3 mg/mL were prepared using 1 % (v/v) acetic acid. TPP solutions with concentrations ranged from 0.5–1.5 mg/mL were prepared by dissolving TPP in ultrapure water and left stirred for 5 min. Then, TPP solution was filtered using 0.20 µm syringe filter. The pH of chitosan solution was adjusted to 4.8 using 1M NaOH solution prior to the addition of TPP. A stabilizer, Tween 80 (0.25% (v/v)) was used and violacein with concentrations ranging from 1–3 ppm were added into the chitosan solution and left stirred for 10 min. The formation of chitosan nanoparticles was carried out by adding TPP as cross-linker dropwise into the mixture of chitosan, Tween 80, and violacein pigment under constant stirring (700 rpm) for 30 min at room temperature (25 ± 2 °C). The suspensions were subsequently centrifuged at 25000 rpm using ultracentrifuge (ThermoFisher Scientific, USA) for 30 min. The resulting suspensions were immediately frozen at -20 °C for approximately 4 h and freeze dried (Alpha 1-2/LD Plus, Germany). All samples were then stored at ± 4 °C prior to analysis.

RSM experimental design

Design Expert Software (Design Expert 7.1.6) was utilized to perform regression and graphical analyses of experimental data obtained during the preparation of violacein pigment nanoparticles. Box-Behnken design (BBD) was chosen based on the selection of three levels for each of four factors namely the concentration of chitosan (A), the concentration of TPP (B), the chitosan:TPP mass ratio (C), and the concentration of violacein pigment (D). BBD was employed to evaluate the main effects, interaction effects, and quadratic effects of the aforementioned factors upon particle size (R_1) and zeta potential (R_2) as responses. A design consisted of 29 runs were developed and a polynomial equation was generated as follows [10]:

$$R = b_0 + b_1A + b_2B + b_3C + b_4D + b_{12}AB + b_{13}AC + b_{14}AD + b_{23}BC + b_{24}BD + b_{34}CD + b_{11}A^2 + b_{22}B^2 + b_{33}C^2 + b_{44}D^2 \quad (1)$$

whereby R is response, b_0 is intercept, and b_1-b_{44} indicate regression coefficient calculated from the observed values of R from the experiments. The interaction and quadratic terms are represented by (AB, AC, AD, BC, BD, and CD) and (A^2, B^2, C^2, and D^2), respectively. The three level design points (low, medium and high) of factors in actual and coded values with their responses are presented in Table 1. Stirring speed, stirring time, and concentration of Tween 80 were fixed at 700 rpm, 1 h, and 0.25 % (v/v), respectively. The design layout consists of 29 experimental formulations of violacein nanoparticles and their observations of factors on the responses are shown in Table 2.

Data analysis, optimization and validation of applied model

Analysis of variance (ANOVA) was used to determine the adequacy of the design model to describe the observed data as well as the significance of factors and their interactions upon the responses. The relative effects of factors on the responses could be estimated based on the magnitude (positive or negative) of regression coefficients of the fitted model. Best fitting experimental model of responses onto either linear, two factorial interaction (2FI), and quadratic was observed and evaluated statistically. The optimization of the violacein pigment nanoparticles were performed by setting the goal of responses attaining the violacein nanoparticles with minimum particle size as well as maximum zeta potential. A check-point analysis was done in order to establish and evaluate the reliability of the developed model.

Characterization of violacein nanoparticles

Physicochemical characterization of violacein nanoparticles were carried out on total of 29 formulations as proposed by RSM.

Table 1 Variables in Box Behnken design (BBD) used for optimization of nano-sized violacein pigment.

Independent variables (Factors)	Units	Actual and coded levels		
		-1	0	+1
A: Concentration of chitosan	mg/mL	1.0	2.0	3.0
B: Concentration of tripolyphosphate (TPP)	mg/mL	0.5	1.0	1.5
C: Chitosan:TPP mass ratio	-	5	6	7
D: Concentration of violacein pigment	ppm	1.0	2.0	3.0
Dependent variables (Responses)	**Units**		**Aims**	
R_1: Particle size	nm		Minimize	
R_2: Zeta potential	mV		Maximize	

Table 2 Measured responses for factors of nano-sized violacein pigment.

Runs	Factors				Responses	
	A (mg/mL)	B (mg/mL)	C	D (ppm)	R_1 (nm)	R_2 (mV)
1	2.0	0.5	6.0	1.0	15.40	23.70
2	2.0	1.5	5.0	2.0	78.98	12.94
3#	2.0	1.0	6.0	2.0	146.53	6.10
4	1.0	1.5	6.0	2.0	103.99	13.70
5	2.0	1.5	6.0	1.0	13.26	23.97
6	2.0	1.0	7.0	2.0	183.43	37.90
7	3.0	1.5	6.0	2.0	97.28	30.53
8#	2.0	1.0	6.0	2.0	222.37	29.70
9	2.0	0.5	5.0	2.0	30.23	22.3
10	2.0	1.5	6.0	3.0	63.58	3.86
11#	2.0	1.0	6.0	2.0	133.47	23.00
12	2.0	1.5	7.0	2.0	132.37	29.90
13	2.0	1.0	5.0	1.0	22.24	9.16
14	3.0	1.0	5.0	2.0	198.93	29.17
15	1.0	1.0	7.0	2.0	223.83	20.07
16#	2.0	1.0	6.0	2.0	198.73	17.40
17	1.0	1.0	5.0	2.0	102.23	7.73
18	1.0	1.0	6.0	1.0	46.61	-0.15
19	3.0	1.0	6.0	3.0	171.18	10.28
20	1.0	0.5	6.0	2.0	152.77	20.77
21	2.0	0.5	7.0	2.0	210.60	20.1
22	2.0	1.0	5.0	3.0	92.53	-0.614
23	2.0	1.0	7.0	3.0	118.54	1.32
24	2.0	1.0	7.0	1.0	97.07	19.1
25	2.0	0.5	6.0	3.0	192.34	11.65
26	1.0	1.0	6.0	3.0	50.64	-2.19
27	3.0	1.0	6.0	1.0	171.60	19.27
28#	2.0	1.0	6.0	2.0	204.03	13.40
29	3.0	0.5	6.0	2.0	284.60	42.43

#: Centre point

Particle size and zeta potential

Particle size distribution and zeta potential of violacein nanoparticles were determined through dynamic light scattering (DLS) by using Zetasizer Nano (Malvern, UK). Freeze-dried violacein nanoparticles were dissolved in 20 mL of ultrapure water and dispersed ultrasonically using probe sonicator (QSonica, USA) for 5 min prior to analysis. Measurements were performed by transferring about 1 mL of the solution into a disposable folded capillary cell. The analysis was then operated at 173º of scattering angle at room temperature (25 ± 2 ℃). The measurement of each samples were done in triplicates.

Morphological analysis using field emission scanning electron microscope (FESEM)

Surface morphologies of violacein nanoparticles and chitosan nanoparticles as blank were observed using FESEM (Hitachi SU8020, Japan). A small drop of the suspension was put onto the stub and left dried in desiccators for 30 min. The stubs containing sample were sputtered and coated with platinum prior to analysis. The image was successfully acquired using electron accelerating voltage of 5 kV at magnification of 100,000.

RESULTS AND DISCUSSION

Data analysis and model fitting

Model fitting of the observed responses (particle size and zeta potential) onto either linear, two factorial interaction (2FI), quadratic, and cubic were analyzed. Several statistical parameters such as standard deviation (SD), multiple correlation coefficient (R^2), adjusted multiple correlation coefficient (adjusted R^2), and predicted multiple correlation coefficient (predicted R^2) were taken into consideration (Table 3). A model with low SD, R^2, and adjusted R^2 value close to 1.0 and adequate precision greater than 4 was selected as best fitting model. From the observations, the particle size and zeta potential were best fitted to the quadratic model as suggested by the Design Expert 7. Cubic model also showed signs of being fit model but it was determined as "aliased" since this model provided unreasonably little points or chooses the wrong points that lead to unstable coefficients and inaccurate graphs. Hence, aliased model (cubic) was not chosen.

The quadratic model was further analyzed for the accuracy of the fit and the significance using ANOVA (Table 4). The R^2, adjusted R^2, and predicted R^2 values for the surface quadratic model of particle size are 0.8250, 0.6499 and 0.1628, respectively. These values are considered lower than values obtained by Abul Kalam *et al.* [12] as the values were 0.9178, 0.8974 and 0.8856, respectively. The effects of chitosan concentration, TPP concentration, and stirring time on the particle size, encapsulation efficiency, and cumulative drug release were analyzed. Despite of the high values of aforementioned statistical parameters, the quadratic model of particle size had significant lack of fit (F-values: 18.04 and p-values: 0.0087). F-values and p-values are important in determining the significance of each coefficient. The corresponding coefficient term is considered to be more significant when magnitude of F-values and p-values are larger and smaller, respectively [23]. The model F-values for R_1 (particle size) and R_2 (zeta potential) are 4.71 and 5.36 respectively, which implied that the model

is significant for both responses. Responses R_1 and R_2 only have 0.32% and 0.17% chances, respectively due to noises. The "lack of fit F-values" of 1.32 for R_1 and 0.32 for R_2 indicates the lack of fit is insignificant relative to the pure error. Lack of fit F-values were large with 42.46 % and 93.53 % chances for R_1 and R2, respectively. Since, non-significant lack of fit was good, quadratic model of particle size in this study is better and the model was found to be fitted.

Table 3 Model summary of statistical parameters.

Response	Models	SD	R^2	Adjusted R^2	Predicted R^2	Remarks
R_1 (nm)	Linear	62.66	0.3606	0.2540	0.0625	
	2FI	65.02	0.4836	0.1968	-0.4213	
	Quadratic	42.93	0.8250	0.6499	0.1628	Suggested
	Cubic	33.41	0.9546	0.7880	0.2593	Aliased
R_2 (mV)	Linear	9.24	0.4484	0.3564	0.1793	
	2FI	10.28	0.4875	0.2027	-0.5029	
	Quadratic	6.46	0.8428	0.6857	0.4621	Suggested
	Cubic	8.71	0.8875	0.4282	-4.1797	Aliased

Table 4 ANOVA for response surface quadratic model.

Terms	Particle size (R_1)			Zeta potential (R_2)		
	F-values	p-value > F	Remarks	F-values	p-value > F	Remarks
Model	4.71	0.0032	Significant	5.36	0.0017	Significant
Linear						
A	8.24	0.0123		24.03	0.0002	
B	7.11	0.0184		1.36	0.2636	
C	8.78	0.0103		4.55	0.0511	
D	4.71	0.0477		10.00	0.0069	
2FI						
AB	2.60	0.1289		0.14	0.7140	
AC	2.55	0.1326		0.08	0.7839	
AD	2.69×10^{-3}	0.9594		0.29	0.5989	
BC	2.19	0.1613		2.20	0.1600	
BD	2.18	0.1624		0.39	0.5426	
CD	0.32	0.5786		0.38	0.5452	
Quadratic						
A^2	0.68	0.4219		1.20	0.2922	
B^2	4.95	0.0430		5.73	0.0313	
C^2	1.87	0.1927		0.01	0.9319	
D^2	21.18	0.0004		18.81	0.0007	
Lack of fit	1.32	0.4246	Insignificant	0.32	0.9353	Insignificant

R_1, R^2: 0.8250; Adjusted R^2: 0.6499;Predicted R^2:0.1628
R_2, R^2: 0.8428; Adjusted R^2: 0.6857;Predicted R^2:0.4621

Table 5 ANOVA for response surface reduced quadratic model.

Terms	Particle size (R_1)			Zeta potential (R_2)		
	F-values	p-value > F	Remarks	F-values	p-value > F	Remarks
Model	6.84	0.0003	Significant	13.80	< 0.0001	Significant
Linear	7.10	0.0145				
A				28.28	< 0.0001	
B	6.12	0.0220		1.60	0.2197	
C	7.56	0.0120		5.35	0.0304	
D	4.05	0.0571		11.77	0.0024	
2FI				-	-	
AC	2.20	0.1533				
Quadratic						
B^2	4.19	0.0533		6.09	0.0219	
D^2	18.68	0.0003		25.63	< 0.0001	
Lack of fit	1.53	0.3688	Insignificant	0.31	0.9630	Insignificant

R_1, R^2: 0.6632; Adjusted R^2: 0.5943; Predicted R^2: 0.4115
R_2, R^2: 0.7901; Adjusted R^2: 0.7329; Predicted R^2: 0.6

The "p-value > F" less than 0.05 indicates that the model terms are significant. As for R_1, the significant terms are A, B, C, D, B^2, and D^2 while for R_2, the significant terms are A, C, D, B^2, and D^2. The values greater than 0.10 indicate that the model terms are not significant and it should be removed from the model as model reduction (Table 5). Additionally, model reduction should also be considered for both responses since the "Predicted R^2" value is not as close to the "Adjusted R^2" as expected where values should be within 0.2. Thus, evaluation of the model adequacy on the basis of the "Adjusted R^2" is necessary [23,24]. Each reduced quadratic model of responses R_1 and R_2 have new values of the "R^2", "Adjusted R^2", and "Predicted R^2" whereby the corresponding values for response R_1 are 0.6632, 0.5943, and 0.4115, respectively. As for reduced model response R_2, new values of the "R^2", "Adjusted R^2", and "Predicted R^2" are 0.7901, 0.7329 and 0.663, respectively. It could be observed for both cases that the "Predicted R^2" and "Adjusted R^2" are in reasonable agreement.

Interaction effects of factors on the responses

In polynomial equations, the interaction and quadratic terms indicated by coefficients with more than one factor and with higher order terms respectively, suggesting the non-linear relationship between the factors and responses [12]. Additionally, the magnitude of coefficients in polynomial equation has either positive and negative sign that signified as synergistic effect and antagonistic effect, respectively, between the factors and responses [13]. The interaction effect of all the factors toward both responses could be observed from the Eq. (2) and (3) as presented in terms of coded factors as shown:

$$\text{Particle size} = +176.05 + 35.58A - 33.04B + 36.73C + 26.89D - 34.27AC - 36.06B^2 - 76.11D^2 \quad (2)$$

$$\text{Zeta potential} = +19.55 + 9.14A - 2.17B + 3.98C - 5.90D + 5.59B2 - 11.47D^2 \quad (3)$$

A, C, and D were found to have synergistic effects on particle size (R_1) while A and C only have synergistic effects on zeta potential (R_2). Factor D was found to have an antagonistic effect with zeta potential but synergistic effect on particle size with high magnitude. The interaction effect of AC was found negative upon particle size. As for the quadratic effect, B^2 and D^2 showed antagonistic effects on particle size whereas quadratic effect of B^2 was found to have a synergistic effect on zeta potential. Based on Eq. (2) and (3) both particle size and zeta potential were primarily affected by factors A and C. This was supported by perturbation plots (Figure 2) which showed sharp slope indicated that both responses were sensitive to factor A and C.

Two-factorial interaction effects of the both factors A (concentration of chitosan) and C (chitosan:TPP mass ratio) on particle size and zeta potential while other two factors B (concentration of TPP) and D (concentration of violacein pigment) was kept constant were observed in Figure 3 and Figure 4 (3D and contour plots). It was observed from 3D surface plots (Figure 3 (a)) that the particle size of nano-sized violacein pigment increased as concentration of chitosan increased from 1.0 to 3.0 mg/mL. Similarly with chitosan:TPP mass ratio as high mass ratio increased the particle size of violacein. Thus, small particle size of nano-sized violacein is produced at low concentration of chitosan and mass ratio chitosan to TPP. The 2D contour plot corresponding to the 3D response surface graph (Figure 3 (b)) indicated that nano-sized violacein pigment with size of 101.62 nm obtained at concentration of chitosan ranging from 1.0 to 1.6 mg/mL with chitosan:TPP mass ratio ranged from 5.0 to 5.7. The results surpassed results reported by Hussain and Sahudin [22] whereby as larger particle size ranged from 122 to 227 nm was obtained at concentration of chitosan ranged from 0.5 to 2.0 mg/mL with constant chitosan:TPP mass ratio of 5:1 [22]. Formulation of larger particle size of violacein pigment (~198 nm) was observed as the concentration of chitosan reached 3.0 mg/mL. This might be due to the partial escalation in intermolecular cross-linking of the nanoparticles as the chitosan molecules keep approaching each other caused by the equilibrium between the interchain hydrogen bonding attraction and intermolecular electrostatic repulsion of the chitosan molecules [12].

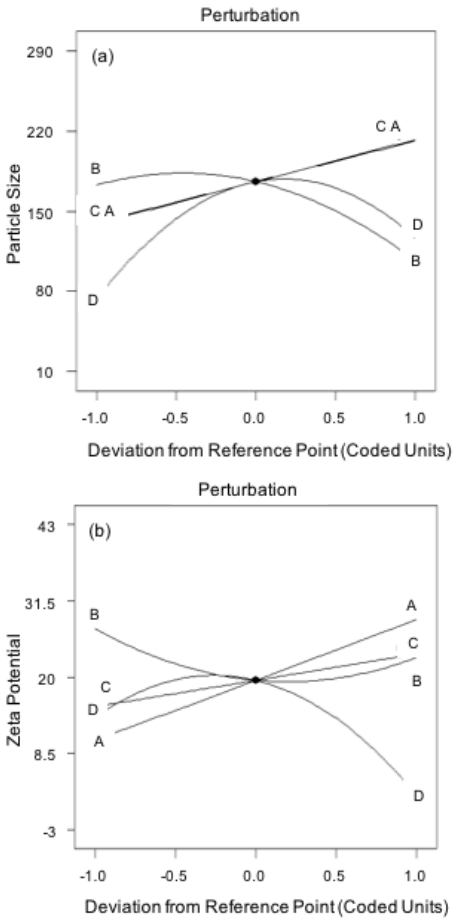

Figure 2 Perturbation plots for (a) particle size (b) zeta potential.

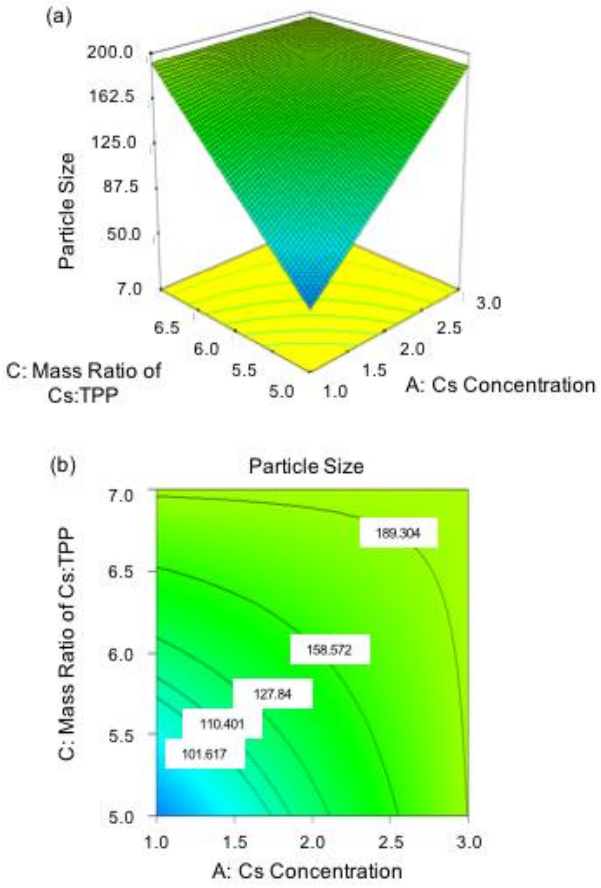

Figure 3 (a) 3D response surface graphs and (b) 2D contour plots illustrating the interaction effect of concentration of chitosan (A) and chitosan:TPP mass ratio (C) on particle size.

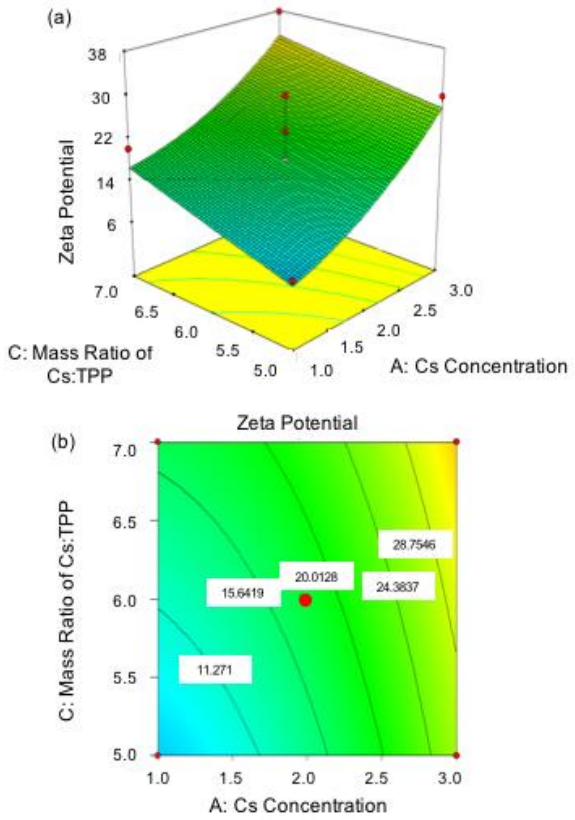

Figure 4 (a) 3D response surface graphs and (b) 2D contour plots illustrating the interaction effect of concentration of chitosan (A) and chitosan:TPP mass ratio (C) on zeta potential.

As for the zeta potential, the 3D response surface graph (Figure 4 (a)) showed that both concentration of chitosan as well as chitosan:TPP mass ratio exhibited similar effects. Increase in concentration of chitosan and chitosan:TPP mass ratio increased zeta potential of violacein nanoparticles. Zeta potential is defined as an electrical charge possessed by the particle on the surface that acts as a repulsive factor which provide stability to formulation [13]. Hence, high zeta potential value is achieved with high concentration of chitosan with large mass ratio of chitosan:TPP. The 2D contour plot of zeta potential (Figure 4 (b)) indicated that violacein pigment nanoparticles with zeta potential of 28.75 mV was obtained at concentration of chitosan of 3.0 mg/mL with chitosan:TPP mass ratio ranged from 5.6 to 7.0. Hussain and Sahudin [22] reported that zeta potential of the chitosan nanoparticles was significantly increased from +19 to +52 mV as when the chitosan concentration was increased from 0.5 to 4 mg/ml. On the other hand, zeta potential linearly increased from +12 to +34 mV when the chitosan:TPP mass ratios were increased from 2:1 to 6:1. However, zeta potential was decreased from +34 to +26 mV as chitosan:TPP mass ratio increased from 6:1 to 10:1 [22].

Data optimization and model validation

Based on the model obtained, it was found that optimal formulation to obtain a predicted 55.21 nm size and 24.82 mV zeta potential of violacein nanoparticles was at concentration of chitosan 2.3 mg/mL, 1.5 mg/mL of TPP, chitosan:TPP mass ratio of 7:1 and 1 ppm of violacein concentration. However, the experimental values of particle size and zeta potential responses were deviated from the predictions as the values are 149 nm for particle size and 23.4 mV for zeta potential (Table 6).

This could be due to the variation error from the extraneous sources such as machine malfunction (freeze-dry) during the preparation process over a period of time [25]. Moreover, chitosan easily degrades due to its high susceptibility to environmental factors and processing conditions that applied stress on its structure [26]. The adequate precision for model particle size is 8.648 and 14.842 for zeta potential indicates that both models can be used to navigate the design space. The adequate precision that measures the signal-to-noise ratio (error) [10,12] for model of both responses were found to be larger than 4 which is desirable for navigating the design space.

Table 6 ANOVA for response surface reduced quadratic model.

Optimized formulation (A:B:C:D)	Responses	Actual value	Predicted value
Formulation 1	Particle size (nm)	149.0	55.21
2.33:1.5:7:1	Zeta potential (mV)	23.40	24.82
Formulation 2	Particle size (nm)	224.60	41.41
2.47:1.5:7:1	Zeta potential (mV)	17.36	25.96
Formulation 3	Particle size (nm)	299.10	41.19
2.41:1.5:7:1	Zeta potential (mV)	8.00	24.96

Morphological analysis using field emission scanning electron microscope (FESEM)

Figure 5 shows FESEM images representing the surface morphology of violacein nanoparticles and chitosan nanoparticles (blank). It is observed that the violacein nanoparticles are in smaller size and uniformly distributed as compared to the blank. The aggregation of particles were observed in the blank and the particles seemed to be large in size.

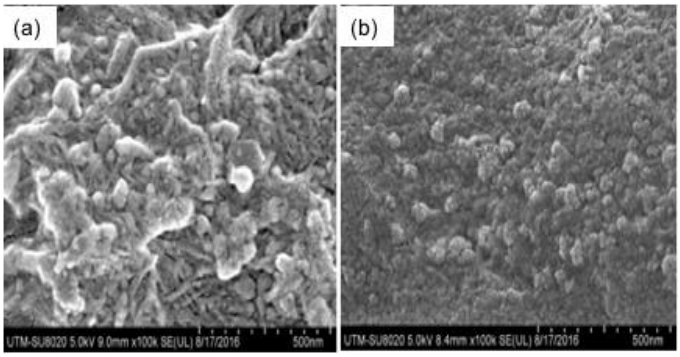

Figure 5 FESEM images of (a) chitosan nanoparticles (b) violacein nanoparticles at 100,000 magnifications.

CONCLUSION

Factors involved in the preparation of nano-sized violacein pigment through encapsulation with chitosan nanoparticles had been optimized using response surface methodology. Particle size of 149 nm and zeta potential of 23.4 mV of violacein pigment nanoparticles were obtained at the optimal formulation of 2.33 mg/mL of chitosan, 1.5 mg/mL of TPP and 1 ppm of violacein pigment with chitosan:TPP mass ratio of 7:1. The violacein pigment nanoparticles were characterized for their morphological structure using FESEM which showed uniform distribution with less aggregation as well as smaller than the blank. The development of nano-sized violacein pigment from this study could improve the solubility of violacein pigment which is known as poorly water-soluble pigment. Additionally, the reduction in size of violacein pigment into nano-scale could minimize its toxicity towards human in order to be applied as an additive and a colorant in various materials such as foods, cosmetics, clothes, ink, paper and so forth. The synthesized of nano-sized violacein pigment can also possibly act as therapeutic agents in the pharmaceutical fields. Moreover, the optimization studies could give ideas on the important preparation parameters to be considered when synthesizing violacein pigment in nano-scale.

ACKNOWLEDGEMENT

This work was financially supported by the Universiti Teknologi Malaysia under the Research University Grant (Q.J130000.2526.12H83) and Ministry of Education Malaysia (R.J130000.7826.4F895).

REFERENCES

[1] Pereira, D. M., Valento, P., Andrade, P. B. 2014. Marine natural pigments: Chemistry, distribution and analysis. *Dye Pigment*, 111:124–134. doi:10.1016/ j.dyepig.2014.06.011.

[2] Venil, C. K., Aruldass, C. A., Dufossé, L., Zakaria, Z. A., Ahmad, W. A. 2014. Current perspective on bacterial pigments: Emerging sustainable compounds with coloring and biological properties for the industry – An incisive evaluation. *RSC Advances*, 4:39523-39529. doi:10.1039/C4RA06162D.

[3] Konzen, M., De Marco, D., Cordova, C. A. S., Vieira, T. O., Antônio, R. V., Creczynski-Pasa, T. B. 2006. Antioxidant properties of violacein: possible relation on its biological function. *Bioorganic and Medicinal Chemistry*, 14:8307–8313. doi:10.1016/j.bmc.2006.09.013.

[4] Azevedo, M. B. M. D., Alderete, J., Jaime, A., Faljoni-alario, A., Haun, M., Duran, N. 2000. Biological activities of violacein, a new antitumoral indole derivative in an inclusion complex with β-Cyclodextrin. *Journal of Inclusion Phenomena and Macrocyclic Chemistry*, 37:93–101.

[5] Andrighetti-Fröhner, C. R., Antonio, R. V., Creczynski-Pasa, T. B., Barardi, C. R. M., Simões, C. M. O. 2003. Cytotoxicity and potential antiviral evaluation of violacein produced by *Chromobacterium violaceum*. *Memorias de Instituto Oswaldo Cruz*, 98:843–848. doi:10.1590/S0074-02762003000600023.

[6] Sasidharan, A., Sasidharan, N. K., Amma, D. B. N. S., Vasu, R. K., Nataraja, A. V., Bhaskaran, K. 2015. Antifungal activity of violacein purified from a novel strain of *Chromobacterium sp.* NIIST (MTCC 5522). *Journal of Microbiology*, 53:694–701. doi:10.1007/s12275-015-5173-6.

[7] Aruldass, C. A., Rubiyatno, R., Venil, C. K., Ahmad, W. A. 2015. Violacein pigment production from liquid pineapple waste by *Chromobacterium violaceum* UTM5 and evaluation of its bioactivity. *RSC Advances*, 5:51524–51536. doi:10.1039/C5RA05765E.

[8] Alshatwi, A. A., Subash-Babu, P., Antonisamy, P. 2016. Violacein induces apoptosis in human breast cancer cells through up regulation of BAX, p53 and down regulation of MDM2. Experimental and Toxicologic Pathology, 68:89–97. doi:10.1016/j.etp.2015.10.002.

[9] Martins, D., Costa, F. T. M., Brocchi, M., Durán, N. 2011. Evaluation of the antibacterial activity of poly-(d,l-lactide-co-glycolide) nanoparticles containing violacein. *Journal of Nanoparticle Research*, 13:355–363. doi:10.1007/s11051-010-0037-9.

[10] Feyzioglu, G. C., Tornuk, F. 2016. Development of chitosan nanoparticles loaded with summer savory (*Satureja hortensis L.*) essential oil for antimicrobial and antioxidant delivery applications. *LWT - Food Science and Technology*, 70:104–10. doi:10.1016/j.lwt.2016.02.037.

[11] Chronopoulou, L., Massimi, M., Giardi, M. F., Cametti, C., Devirgiliis, L. C., Dentini, M. 2013. Chitosan-coated PLGA nanoparticles: A sustained drug release strategy for cell cultures. *Colloids Surfaces B Biointerfaces*, 103:310–317. doi:10.1016/j.colsurfb.2012.10.063.

[12] Abul Kalam, M., Khan, A. A., Khan, S., Almalik, A., Alshamsan, A. 2016. Optimizing indomethacin-loaded chitosan nanoparticle size, encapsulation, and release using Box-Behnken experimental design. *International Journal of Biological Macromolecules*, 87:329–340. doi:10.1016/j.ijbiomac. 2016.02.033.

[13] Shah, B., Khunt, D., Misra, M., Padh, H. 2016. Application of Box-Behnken design for optimization and development of quetiapine fumarate loaded chitosan nanoparticles for brain delivery via intranasal route. *International Journal of Biological Macromolecules*, 89:206–218. doi:10.1016/j.ijbiomac. 2016.04.076.

[14] Hashad, R. A., Ishak, R. A. H., Geneidi, A. S., Mansour, S. 2016. Methotrexate loading in chitosan nanoparticles at a novel pH: Response surface modeling, optimization and characterization. *International Journal of Biological Macromolecules*, 91:630–639. doi:10.1016/j.ijbiomac.2016.06.014.

[15] Gulati, N., Nagaich, U., Saraf, S. A. 2013. Intranasal delivery of chitosan nanoparticles for migraine therapy. *Scientia Pharmaceutica*, 81:843-854. doi:10.3797/scipharm.1208-18.

[16] Mitra, S., Gaur, U., Ghosh, P. C., Maitra, A. N. 2001. Tumour targeted delivery of encapsulated dextran-doxorubicin conjugate using chitosan nanoparticles as carrier. *Journal of Controlled Release*. 74:317–323. doi:10.1016/ S0168-3659(01)00342-X.

[17] Gokce, Y., Cengiz, B., Yildiz, N., Calimli, A., Aktas, Z. 2014. Ultrasonication of chitosan nanoparticle suspension: Influence on particle size. *Colloids Surfaces A: Physicochemical and Engineering Aspects*, 462:75–81. doi:10.1016/j.colsurfa.2014.08.028.

[18] Santos, D. T., Meireles, M. A. 2010. Carotenoid pigments encapsulation: fundamentals, techniques and recent trends. *The Open Chemical Engineering Journal*, 4:42–50. doi:10.2174/1874123101004020042.

[19] de Pinho Neves, A. L., Milioli, C. C., Müller, L., Riella, H. G., Kuhnen, N. C., Stulzer, H. K. 2014. Factorial design as tool in chitosan nanoparticles development by ionic gelation technique. *Colloids Surfaces A: Physicochemical and Engineering Aspects*, 445:34–9. doi:10.1016/ j.colsurfa.2013. 12.058.

[20] Myers, R. H., Montgomery, D. C., and Anderson-Cook, C. M. 2016. *Response surface methodology: Process and product optimization using designed experiments*. 4th ed. John Wiley & Sons., Hoboken, New Jersey.

[21] Ahmad, W. A., Yusof, N. Z., Nordin, N., Zakaria, Z. A., Rezali, M. F. 2012. Production and characterization of violacein by locally isolated *Chromobacterium violaceum* grown in agricultural wastes. *Applied Biochemistry and Biotechnology*, 167:1220–1234. doi:10.1007/s12010-012-9553-7.

[22] Hussain, Z., Sahudin, S. 2016. Preparation, charactersation and colloidal stability of chitosan-tripolyphisphate nanoparticles: Optimisation of formulation and process parameters. *International Journal of Pharmacy and Pharmaceutical Sciences*, 8:297-308.

[23] Rahimi, S., Moattari, R. M., Rajabi, L., Ashraf, A. 2015. Optimization of lead removal from aqueous solution using goethite/chitosan nanocomposite by response surface methodology. *Colloids Surfaces A: Physicochemical and Engineering Aspects*, 484:216–225. doi:10.1016/j.colsurfa.2015.07.063.

[24] Luo, X., Guan, R., Chen, X., Tao, M., Ma, J., Zhao, J. 2014. Optimization on condition of epigallocatechin-3-gallate (EGCG) nanoliposomes by response surface methodology and cellular uptake studies in CaCo-2 cells, *Nanoscale Research Letters*, 2014:1–9.

[25] Khuri, A. I., Mukhopadhyay, S. 2010. Response surface methodology. *Wiley Interdisciplinary Reviews (WIREs)*, 2:128–149. doi: 10.1002/wics.73.

[26] Szymańska, E., Winnicka, K. 2015. Stability of chitosan - A challenge for pharmaceutical and biomedical applications. *Marine Drugs*, 13:1819–1846. doi:10.3390/md13041819.